

IGNITION CHARACTERISTICS OF TURBULENT JET FLOWS

R. F. Alvani and M. Fairweather

Department of Chemical Engineering, School of Process, Environmental and Materials Engineering, University of Leeds, Leeds LS2 9JT, UK

Abstract – Releases of flammable materials from chemical plant are a hazard since their dispersion down to safe levels only occurs at some distance from their source. Within this distance, accidental ignition can give rise to fires or explosions. This paper describes the development of computational fluid dynamic models capable of predicting the ignition hazards presented by turbulent releases of flammable materials. A mathematical model, based on solutions of the fluid flow equations, is described, with a prescribed probability density function (p.d.f.) approach used to determine the distribution of conserved scalar quantities. Three distributions are explored, and their ability to simulate experimental data in jet and wake flows, in isolation of fluid flow calculations, is tested. A composite p.d.f. (consisting of **b**- and **d**- functions, and a power law distribution for the viscous super-layer) demonstrates excellent agreement with data, particularly in those regions of a flow that contain significant intermittency. Coupling of this p.d.f. with flow field calculations yields reasonable predictions of scalar p.d.f.'s in a methane jet, with probabilities of ignition implied from measured and predicted p.d.f.'s being in close accord. The results demonstrate that prescribed p.d.f. methods are likely to be capable of predicting ignition probabilities in many practical flows.

Keywords – Flammable materials, dispersion, ignition probability, computational fluid dynamics, prescribed probability density function.

INTRODUCTION

Safety issues are paramount in all the operations that any organisation undertakes. Within the UK, legislation means that organisations have a duty to ensure, as far as is reasonably practicable, the safety of employees and members of the public who might be affected by their operations. In the case of major hazard installations, this also entails the submission of safety reports. Past research in the safety area has improved the quality of life within the UK through increased safety and reduced risk to the public and plant operators. This work has also been of significant benefit to the competitiveness of UK industry in reducing the cost of expensive safety-related equipment, allowing the design of more compact plant, and decreasing insurance costs.

Despite the importance of safety, however, major incidents continue to occur. The total cost of onshore accidents in the UK chemical and petrochemical sectors in the 22 years following the Flixborough incident in 1974 is conservatively estimated^{1, 2} (in 1996 values) at £500 M. Lack of data means that there is much uncertainty in this figure, with the true value possibly being a factor of 2 or more higher¹. This figure also excludes offshore incidents such as the Piper Alpha tragedy that occurred in 1988, which claimed 165 lives. Home Office statistics for 1997 show that fires alone in the UK claimed 730 lives and injured 18,600. The total cost is estimated at £5 Billion per year, or approximately 1% of GDP, with figures for 1993 showing that non-domestic fires cost £1.2 Billion in terms of losses to business, property and victims in that year alone.

The operational or accidental release of flammable materials represents a major hazard to the public, industrial plant and plant operators since the dispersion of these materials down to

non-flammable levels only occurs at some distance from the source of material. Within this distance, accidental ignition can give rise to fires or explosions. Hazardous area classification (HAC) is used to establish the safe distances around any release, and to identify those areas where control of electrical equipment and other ignition sources is necessary. It also allows the requirements for ventilation to be assessed. HAC is applied in a diverse range of situations covering releases from pressurised sources, leaks and spills: on offshore rigs and chemical plants at the largest scales, in factories and other commercial operations, to gas cylinder stores and small garages at the smallest scale. In addition, safety reports on chemical and process plant, and transportation systems such as pipelines, demand that predictions be made of the dispersing jets or plumes that arise should an accidental release of flammable material occur. Similar assessments also need to be performed for operational (e.g. vents) and emergency releases. These predictions are in turn employed to assess likely hazards to personnel and plant from the existence of flammable clouds.

Current codes of practice for HAC are based almost entirely on judgement and past experience, and there is overwhelming evidence that they are over prescriptive and entail excessive costs to UK industry. Safety cases undertaken for major hazard sites, and safety recommendations, similarly rely heavily on custom and practice, or on conservative predictions based on the mean concentrations of flammable material around the source, which again entails excessive costs. This over-conservatism leads to hazardous areas that are too extensive, committing industry to considerable expense in making such areas safe or in providing sterile areas in and around plant. This leads to the cancellation, or transfer to other countries, of new manufacturing projects and extensions to existing facilities, the adoption of unrealistic constraints on operational throughput, and the adoption of unrealistic emergency plans, all of which significantly reduces the competitiveness of UK industry, or discourages the development of manufacturing within the UK.

There is therefore a requirement for scientific methods for calculating the dispersion and ignitability of flammable materials from open pools and pressurised sources, and for convincing validation of the techniques developed against reliable experimental data. Computational fluid dynamics offers the potential for providing a cost-effective means of assessing the hazards around any release, of establishing any requirements for ventilation, and of providing detailed predictions for realistic and complex release scenarios. Indeed, such techniques have already been applied to calculating the dispersion of material from jet and pool releases, both within buildings and outdoors.

When used at all these, and simpler modelling techniques, are employed to predict mean concentration fields from which hazardous zones are determined. For the vast majority of releases encountered in practice, however, the existence of a pressurised or large diameter source means that flow Reynolds numbers are turbulent. In such flows, it is known that the flammability of the mixture (i.e. whether it will ignite or not) is not related to the mean concentration field, and that assessments of those locations where ignition may occur should be based on a statistical knowledge of local flow conditions. In particular, it is necessary to know the probability density function (p.d.f.) of the flammable material in air at all locations around the release to allow identification of those positions where flammable mixture exists. In addition, in those regions where an ignition can occur, the flame formed may or may not light-up the source material, i.e. in some situations light-up will occur, but in others the flame formed locally will be extinguished. Current safety and hazard analyses avoid these issues, but ensure conservatism by basing assessments of those locations where ignition and/or light-

up can occur on predictions of very low mean concentration levels. As noted above, this results in over-prescriptive recommendations, and causes unnecessary expense for industry. In addition, however, assessments based on mean concentrations do not reflect the physics of the processes that govern ignitability, and as such cannot be guaranteed to be safe under all circumstances.

The work described in this paper represents the initial stages of an ongoing programme aimed at the development of computational fluid dynamic models capable of predicting the ignition hazards presented by turbulent releases of flammable materials. At this stage of development, predictions of the flow field associated with a dispersing release have been obtained by solutions of the fluid flow equations, coupled to statistical engineering turbulence models. Probability density functions of scalar quantities within the flow have been obtained by prescribing their shape, with their subsequent integration over the flammable range of released material being used to derive probabilities of ignition. The work described also focuses on turbulent jet releases since data for model validation is generally only available for such simple flows.

MATHEMATICAL MODEL

TURBULENT FLOW CALCULATIONS

The jet studied experimentally³, and for which ignitability information is available, was essentially parabolic and axisymmetric. Predictions were therefore derived from solutions of the partial differential equations which describe conservation of mass, momentum (including buoyancy terms) and conserved scalar (mixture fraction) transport. For the variable density flows of interest, density weighted (Favre) averaged forms of these equations were employed. Closure of this equation set, through modelling of the unknown Reynolds stress and turbulent scalar flux terms, was achieved using either a k- ϵ approach⁴ or a full second moment closure⁵.

In the former approach, the Reynolds stress was specified as linearly related to the mean rate of strain via a scalar turbulent viscosity, and the turbulent scalar flux obtained using a gradient diffusion model. Transport equations for the turbulence kinetic energy, the dissipation rate of turbulence energy and the variance of mixture fraction were then solved. Various modifications to standard values⁶ of the modelling constants were examined to improve spreading rate predictions of the round jet of interest, including variations in $C_{\epsilon 1}$ and the $C_{\epsilon 1}$ modification proposed by Syed⁷. Closest agreement was obtained using a value of $C_{\epsilon 1} = 1.48$, and this value was retained in all the predictions given below.

In the second moment turbulence closure the Reynolds stresses and turbulent scalar flux were obtained directly from solutions of modelled partial differential transport equations. These equations were as specified by Jones and Musonge⁵ for the Reynolds stresses, although an improved version⁸ of the scalar flux model was employed. Modelling constants were again examined, with those employed by Jones and Musonge⁵ and Dianat et al.⁹ being explored, as well as modifications to $C_{\epsilon 2}$. Closest agreement with data was obtained using a value⁸ of $C_{\epsilon 2} = 1.80$, and this value was used in all predictions considered in later sections.

Solution of the appropriate axisymmetric forms of the transport equations was achieved using a modified version of the GENMIX¹⁰ code. In the absence of suitable experimental data, the jet was assigned initial mean velocity and turbulence quantities typical of fully developed

turbulent pipe flow¹¹. Both flat and profiled initial conditions were examined, with profiled values resulting in best agreement with data. Numerical solutions were obtained using expanding finite-volume meshes in both the axial and radial directions, with 610×200 nodes in the downstream and radial directions, respectively, being found sufficient to give predictions that were free of numerical error.

As noted above, buoyancy effects were accommodated in the modelled equations. Buoyancy can, however, also influence the turbulence field, and such effects were examined for the k- ϵ model using the modifications described by Jones and Ledin¹², and for the second moment closure using the terms suggested by Jones and Musonge⁵. In all cases, predictions incorporating buoyancy effects were negligibly different from those which excluded such effects.

PRESCRIBED PROBABILITY DENSITY FUNCTIONS

Local concentration probability density functions within the flow were evaluated by prescribing a shape for the p.d.f., with the probability of ignition then being derived by integration over the p.d.f. between the lower and upper static flammability limits of the jet fluid.

A number of different shaped distributions have been used in the past to model the conserved scalar, although the **b**-function distribution assumed by Richardson et al.¹³ is the most widely used today. The parameters that define this function can be specified directly from the first two moments of the mixture fraction, obtained from solution of their transport equations. Predictions were obtained using this p.d.f., which can be written as:

$$P^I(f) = \frac{f^{a-1}(1-f)^{b-1}}{[\Gamma(\mathbf{a})\Gamma(\mathbf{b})]/[\Gamma(\mathbf{a} + \mathbf{b})]}$$

where Γ is the gamma function and the exponents are given by:

$$\mathbf{a} = \tilde{f} \left(\frac{\tilde{f}(1-\tilde{f})}{\tilde{f}^2} - 1 \right) \text{ and } \mathbf{b} = \mathbf{a} \frac{(1-\tilde{f})}{\tilde{f}}.$$

Measurements of concentration p.d.f.'s obtained³ in a turbulent free jet of methane demonstrate close to Gaussian behaviour along the centre-line of the jet. Moving radially away from the centre-line then gives a broadening concentration distribution with increasing displacement, until the p.d.f. is no longer Gaussian but bimodal, with a high probability of zero concentration. At greater radial displacements this effect becomes more pronounced due to the effects of intermittency. Such intermittency effects cannot be accommodated by the **b**-function p.d.f., although they are significant³ in determining the overall shape of the p.d.f., particularly towards the radial edge of a jet, and hence the probability of ignition at such locations¹⁴. Two other prescribed p.d.f.'s were therefore explored.

The two-part probability density function used by Janicka and Peters¹⁵ comprises a **b**-function for the turbulent part of the flow plus an intermittency spike, modelled using a **d**-function:

$$P^{II}(f) = (1-g)\mathbf{d}(f) + gP^I(f)$$

This p.d.f. therefore accounts for intermittency effects in the outer regions of the turbulent flow. Evaluation of the p.d.f. was again carried out using local values of the mean and variance of mixture fraction, obtained from solution of their transport equations, although

values for the intermittency factor \mathbf{g} are also now required. In the present work these were obtained from the formula proposed by Kent and Bilger¹⁶:

$$\mathbf{g} = \frac{(K + 1)}{\left(\frac{\tilde{f}^{n_2}}{\tilde{f}^2} + 1\right)}$$

where K is a constant, taken¹⁶ to be 0.3.

Effelsberg and Peters¹⁷ also proposed a three-part probability density function for conserved scalars, based on a physical interpretation of the turbulence signal obtained within the turbulent part of an intermittent flow. The scalar signal was split into three parts: a fully turbulent part, a super-layer part, and an outer flow part. Each part is then represented by a different part of the p.d.f., and a composite p.d.f. obtained by adding these parts together:

$$P^{III}(f) = (1 - \mathbf{g})\mathbf{d}(f) + \mathbf{g}(sP_s(f) + (1 - s)P^I(f)),$$

where \mathbf{d} - and \mathbf{b} -functions are again used for the outer flow and fully turbulent parts, respectively, and the super-layer part, which occurs within the viscous super-layer where the signal drops from the turbulent value down to zero, modelled according to:

$$P_s(f) = \frac{1 - k}{f^k} I(f)$$

where

$$I = \int_f^1 f^{k-1} P^I(f) df$$

Here, the super-layer factor s and the constant k , which is used in defining the super-layer profile, were derived both from an iterative process based on solutions of expressions for the first four moments of the mixture fraction¹⁷, and from relationships between these parameters and the intermittency factor developed by Effelsberg and Peters¹⁷:

$$s = (1 - \mathbf{g}^2)^{0.25}$$

$$k = 1 - \mathbf{g}^2$$

Whilst the latter expressions are not expected to apply universally¹⁷, they do display a general tendency and, in the present work, were found to lead to more accurate results than when using the alternative iterative calculation method. This is most likely due to inaccuracies in predicted mean and variance of mixture fraction values required, together with intermittency factors, in the latter approach. The results reported below were therefore all derived on the basis of the relationships for s and k given above, with the formula given earlier for the intermittency factor again being employed in this model.

RESULTS AND DISCUSSION

Before considering the ability of the mathematical models outlined above to predict ignition probabilities in releases of flammable materials, it is first useful to assess the accuracy of the various forms of p.d.f. described in representing measured scalar p.d.f.'s in a range of relevant turbulent flows.

Figure 1 shows predictions obtained using the three forms of p.d.f., and scalar p.d.f. profiles measured by LaRue and Libby¹⁸ in the wake behind a heated cylinder at $z/d = 400$ and $Re = 2800$. These data represent some of the best available scalar p.d.f. profiles, for which experimental measurements of \tilde{f} , \tilde{f}^{n_2} , \mathbf{g} , s and k are all available. Importantly, this allows an evaluation of the ability of the various forms of p.d.f. employed to predict measured profiles,

independent of both the p.d.f. modelling assumptions made above, and the fluid flow calculations.

Figure 1 a) to f) shows the comparison between the calculated pd.f.'s and data. Close to the centre-line of the flow (Figure 1 a)), where the flow is fully turbulent, all three p.d.f.'s give good agreement with the data. Moving radially away from the centre-line, Figure 1 b) to f), the measured p.d.f.'s take on a bimodal distribution, with intermittency effects becoming significant at the last four measurements stations. In line with the earlier findings of Effelsberg and Peters¹⁷, the three-part p.d.f. is found to be in excellent agreement with the data at all the measurement stations considered. In contrast, both the two-part and **b**-function p.d.f. fail to capture the overall qualitative shape of the measured p.d.f.'s at all but the first, close to centre-line, location where intermittency effects are negligible.

Measurements of scalar p.d.f.'s along the centre-line and radially within a turbulent, non-reacting propane jet have been obtained by Schefer and Dibble¹⁹. For this jet, measurements of \tilde{f} , \tilde{f}''^2 and \mathbf{g} are available, although for the three-part p.d.f. values of s and k had to be obtained from the formulae given above. Figure 2 compares measured and predicted pd.f.'s along the centre-line of the jet and in all cases, since intermittency effects are negligible at all locations, excellent agreement with the data is obtained for the three predicted forms (with the predictions collapsing onto a single line). This is not the case for the radial locations shown in Figure 3, however, where intermittency effects are again found to become significant for the last four radial locations. Overall, all three forms of pd.f. perform reasonably well, with the three-part p.d.f. being in closest accord with data at the extreme edges of the jet. In Figure 3 c) and d), however, at intermediate radial locations, the super-layer and outer flow parts of the composite p.d.f. tends to be overestimated, with the alternative p.d.f. forms being in closer accord with the data. The two-part p.d.f. is also qualitatively correct in terms of its shape since it exhibits the growing influence of intermittency effects at $f = 0$. This error in the composite p.d.f. predictions is most likely caused by inaccuracies in the s and k values employed in the calculations.

Lastly, Birch et al.³ measured scalar p.d.f.'s at various radial locations in a methane jet. In this case, experimental data for \tilde{f} and \tilde{f}''^2 are available, although values for \mathbf{g} , s and k required by the two- and three-part p.d.f.'s had to be calculated by the methods described earlier. Figure 4 compares measurements and predictions, with little difference between the various predictions being apparent close to the centre-line of the jet (Figure 5 a) and b)). At locations within the intermittent region of the flow (Figure 5 c) and d)), however, the composite p.d.f. is seen to produce the best results. Surprisingly, all the p.d.f.'s fail to reach the correct $P(f)$ maxima in the fully turbulent region of Figure 5 a) to c), but this may be explicable in terms of inaccuracies in the mean mixture fraction data available.

All the above comparisons serve to establish the accuracy of the various prescribed p.d.f.'s in the absence of inaccuracies that inevitably occur when input to their prescriptions is obtained from flow field calculations. In particular, comparisons with the data of Effelsberg and Peters¹⁷, where all the information required as input to calculations of the various p.d.f.'s is available from data, demonstrate the superiority of the three-part p.d.f. Comparisons with the data of Schefer and Dibble¹⁹ and Birch et al.³ also tend to confirm this finding, although larger deviations between measurements and predictions are apparent in these cases due to the requirement by the two- and three-part p.d.f.'s for information that is not available from

measurements. Because of these findings, the predictions given below were based exclusively on the three-part p.d.f.

As well as measuring concentration p.d.f.'s within a jet, Birch et al.³ also obtained data on the mean and variance of mixture fraction in the same methane jet which issued from a 12.65 mm diameter circular pipe at $Re = 1600$. This complete data set permits an evaluation of the ability of coupled flow field and scalar p.d.f. calculations to predict ignition probabilities by comparison of values obtained by integration across the measured¹⁴ and predicted p.d.f.'s.

Figure 5 compares measurements and predictions of centre-line and radial distributions of the mean and variance of mixture fraction within this methane jet (where measurements and predictions are both Favre-averaged). Radial distributions obtained at three axial locations ($z/d = 20, 30$ and 40) have been collapsed in this figure through use of the profile half-width, $r_{1/2}$. Overall, both the $k-\epsilon$ and Reynolds stress closures are seen to provide reasonable predictions of the flow field. Results for the second-moment closure do tend to over estimate mean mixture fraction data up to $z/d = 20$, with mixture fraction variance predictions also being displaced in the downstream direction when compared to the data, resulting in an over prediction of values at those axial locations at which radial profiles are available. This then results in an under prediction of radial variance profiles when expressed in the normalised form given. Overall, however, these predictions are of an accuracy that would be anticipated for circular jets, and sufficiently in-line with the data to permit a meaningful evaluation of the coupled models' ability to predict ignition probabilities.

Figure 6 shows measured and predicted p.d.f.'s at the four radial locations within the Birch et al.³ methane jet considered earlier. In comparison to the three-part p.d.f. results of Figure 4, use of flow field predictions to specify mean and variance of mixture fraction information is seen to result in a deterioration of the predictions close to the centre-line of the jet (Figure 6 a) and b)), where the Reynolds stress model inaccuracies noted earlier lead to significant deviations from experiment. Predictions obtained using both turbulence models improve towards the outer radial regions of the jet, although in Figure 6 c) the Reynolds stress model is seen to significantly overestimate the influence of intermittency.

Integrating the experimental and predicted p.d.f.'s over the flammable range of methane leads to the probabilities of ignition given in Table 1.

Table 1. Measured and predicted probabilities of ignition at various radial locations in the Birch et al. jet at $z/d = 10$.

r/d	Measured	Predicted		
		<i>b</i> -p.d.f	Two-part p.d.f.	Composite p.d.f.
0.00	0.00	0.00	0.00	0.00
1.30	0.21	0.19	0.19	0.19
1.49	0.39	0.31	0.29	0.35
1.80	0.30	0.40	0.29	0.26

Despite the inaccuracies in the predicted p.d.f.'s noted above, results obtained from the composite p.d.f. are seen to be in reasonable agreement with ignition probabilities implied from measurements, with the integration inevitably resulting in an averaging effect which

reduces the influence of predicted errors in the p.d.f. shape. Nevertheless, the maximum error obtained is only 13%, which is likely to be sufficiently accurate for many practical applications. Table 1 also includes equivalent results derived from the **b**-function and two-part p.d.f.'s, with the maximum deviation from data in these cases being, respectively, 33% and 26%. As might be anticipated, all three p.d.f.'s yield ignition probabilities that compare favourably with data close to the centre-line where intermittency effects are small, but in general the two simpler formulations fail to capture the influence of such effects in the outer regions of the flow.

CONCLUSIONS

Of all the presumed shaped p.d.f.'s examined in this investigation, it can be concluded that the three-part p.d.f. performs best, particularly when accurate data is used in its specification. Both the **b**-function and two part p.d.f.'s performed well near the centre-line of the flows examined, but are unable to capture the correct scalar distribution once intermittency effects become significant. Coupling of the three-part p.d.f. with flow field calculations based on both eddy viscosity and second-moment turbulence closures again yields reasonable predictions of scalar p.d.f.'s in the methane jet studied by Birch et al.³, with probabilities of ignition implied by the measured and predicted p.d.f.'s being in close accord. Despite being at the proof-of-concept stage, the results presented demonstrate that prescribed p.d.f. methods are likely to be capable of predicting ignition probabilities in many practical flows.

As the first stage in the development of accurate methods for the prediction of ignition probability, however, further work remains to be performed. In particular, and for developments based on prescribed p.d.f. techniques, it is necessary to develop predictive methods for the intermittency function, rather than relying on the empirical correlation used in the present work. This is one of the most important factors in determining the shape of the three-part p.d.f. as it is used to decide the proportion of each function (power law, \ddot{a} and \hat{a}) employed, as well as being used in the evaluation of the super-layer constants. It is therefore necessary to develop a predictive capability for \mathbf{g} ; with the k- ϵ - γ model of Cho and Chung²⁰ offering the potential not only for the accurate determination of intermittency within an eddy viscosity modelling framework, but also the basis for including such effects within higher order turbulence closures. The application of transported p.d.f. approaches, in which the scalar p.d.f. is predicted from its own transport equation, is also warranted.

NOMENCLATURE

C_{e1}, C_{e2}	Turbulence model constants
d	Pipe diameter
\tilde{f}	Favre-averaged mean mixture fraction
\tilde{f}''^2	Favre-averaged mixture fraction variance
f, f_{cl}	Favre-averaged local and centre-line mean mixture fraction
f', f'_{cl}	Favre-averaged local and centre-line mixture fraction variance
k	Turbulence kinetic energy, super-layer profile constant
l_c	Cylinder length
$P(f)$	Probability density function
r	Radial distance
$r_{1/2}$	Profile half-width
s	Super-layer factor
z	Axial distance

g Intermittency factor
e Dissipation rate of turbulence kinetic energy

REFERENCES

1. Fewtrell, P. and Hirst, I.L., 1998, A review of high cost chemical/petrochemical accidents since Flixborough 1974, *I.Chem.E. Loss Prevention Bulletin* 140:3.
2. Duguid, I.M., 1998, Analysis of past incidents in the oil, chemical and petrochemical industries, *I.Chem.E. Loss Prevention Bulletin* 143:3.
3. Birch, A.D., Brown, D.R., Dodson, M.G. and Thomas, J.R., 1978, The turbulent concentration field of a methane jet, *J. Fluid Mech.* 88:431.
4. Jones, W.P. and Launder, B.E., 1972, The prediction of laminarization with a two-equation model of turbulence, *Int. J. Heat Mass Transfer* 5:301.
5. Jones, W.P. and Musonge, P., 1988, Closure of the Reynolds stress and scalar flux equations, *Phys. Fluids* 31:3589.
6. Jones, W.P. and Whitelaw, J.H., 1982, Calculation methods for turbulent reacting flows, *Combust. Flame* 48:1.
7. Syed, K. J., 1991, Soot and radiation modelling in buoyant fires, Cranfield Institute of Technology, Ph.D. thesis.
8. Fairweather, M., Jones, W.P., Ledin, H.S. and Lindstedt, R.P., 1992, Predictions of soot formation in turbulent, non-premixed propane flames, *Proc. Combust. Inst.* 24:1067.
9. Dianat, M., Fairweather, M. and Jones, W.P., 1996, Reynolds stress closure applied to axisymmetric, impinging turbulent jets, *Theoret. Comput. Fluid Dynamics* 8:435.
10. Spalding, D.B., 1977, *GENMIX: A general computer program for two-dimensional parabolic phenomena*, Pergamon Press, London.
11. Hinze, J.O., 1977, *Turbulence*, McGraw-Hill, New York.
12. Jones, W.P. and Ledin, H.S., 1990, The calculation of a strongly buoyant turbulent diffusion flame, *First Int. Symp. Eng. Turb. Model. and Meas.*, Dubrovnik, Yugoslavia.
13. Richardson, J. N, Howard, H. C. and Smith, R. W., 1953, The relation between sampling-tube measurements and concentration fluctuations in a turbulent gas jet, *Proc. Combust. Inst.* 4:814.
14. Birch, A.D., Brown, D.R. and Dodson, M.G., 1981, Ignition probabilities in turbulent mixing flows, *Proc. Combust. Inst.* 18:1775.
15. Janicka, J. and Peters, N., 1982, Prediction of turbulent jet diffusion flame lift-off using a pdf transport equation, *Proc. Combust. Inst.* 19:367.
16. Kent, J.H. and Bilger, R.W., 1977, The prediction of turbulent diffusion flame fields and nitric oxide formation, *Proc. Combust. Inst.* 16:1643.
17. Effelsberg, E. and Peters, N., 1983, A composite model for the conserved scalar pdf, *Combust. Flame* 50:351.
18. LaRue, J.C. and Libby, P.A., 1974, Temperature fluctuations in the plane turbulent wake, *Phys. Fluids* 17:1956.
19. Schefer, R. W., and Dibble, R. W., 2001, Mixture fraction field in a turbulent non-reacting propane jet, *AIAA Jl.* 39:64.
20. Cho, J. R. and Chung, M. K., 1992, A $k-\epsilon$ equation turbulence model, *J. Fluid Mech.* 237:301.

ACKNOWLEDGEMENT

The authors would like to thank the School of Process, Environment and Materials Engineering at the University of Leeds for its financial support of the work described.

ADDRESS

Correspondence concerning this paper should be addressed to Dr. M. Fairweather, Department of Chemical Engineering, School of Process, Environmental and Materials Engineering, University of Leeds, Leeds LS2 9JT, UK (E-mail m.fairweather@leeds.ac.uk).

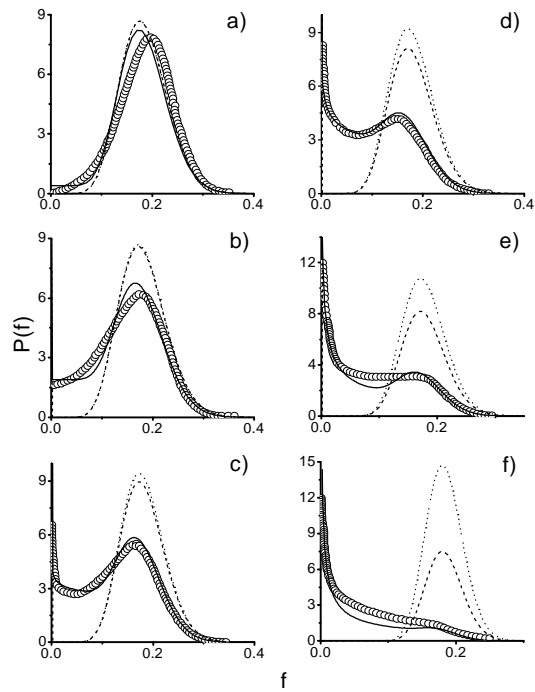


Figure 1. Measured and predicted mixture fraction p.d.f.'s for LaRue and Libby wake flow: a) $r/l_c = 0.028$; b) $r/l_c = 0.162$; c) $r/l_c = 0.209$; d) $r/l_c = 0.257$; e) $r/l_c = 0.294$; f) $r/l_c = 0.349$ (circles – data, solid line – composite p.d.f., dashed line – two-part p.d.f., dotted line – **b**-p.d.f.).

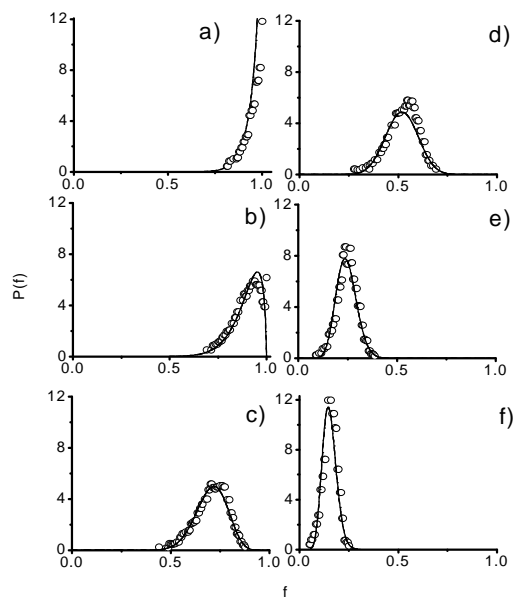


Figure 2. Measured and predicted mixture fraction p.d.f.'s along centre-line of Schefer and Dibble jet: a) $z/d = 5.2$; b) $z/d = 7.1$; c) $z/d = 10.8$; d) $z/d = 15.0$; e) $z/d = 30.0$; f) $z/d = 64.0$ (key as Figure 1).

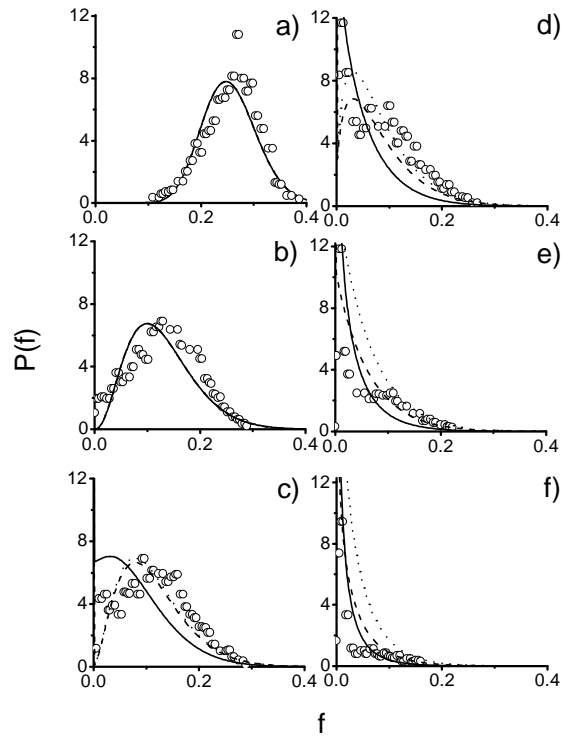


Figure 3. Measured and predicted mixture fraction p.d.f.'s along radius of Schefer and Dibble jet at $z/d = 30$: a) $r/d = 0.0$; b) $r/d = 2.0$; c) $r/d = 2.3$; d) $r/d = 2.6$; e) $r/d = 2.9$; f) $r/d = 3.2$ (key as Figure 1).

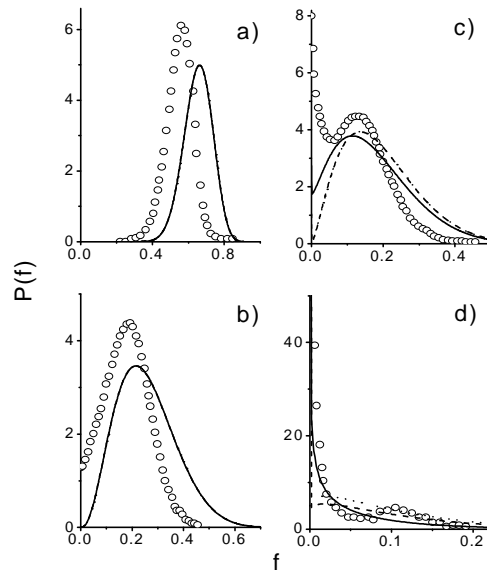


Figure 4. Measured and predicted mixture fraction p.d.f.'s along radius of Birch et al. jet at $z/d = 10$: a) $r/d = 0.0$; b) $r/d = 1.3$; c) $r/d = 1.49$; d) $r/d = 1.8$ (key as Figure 1).

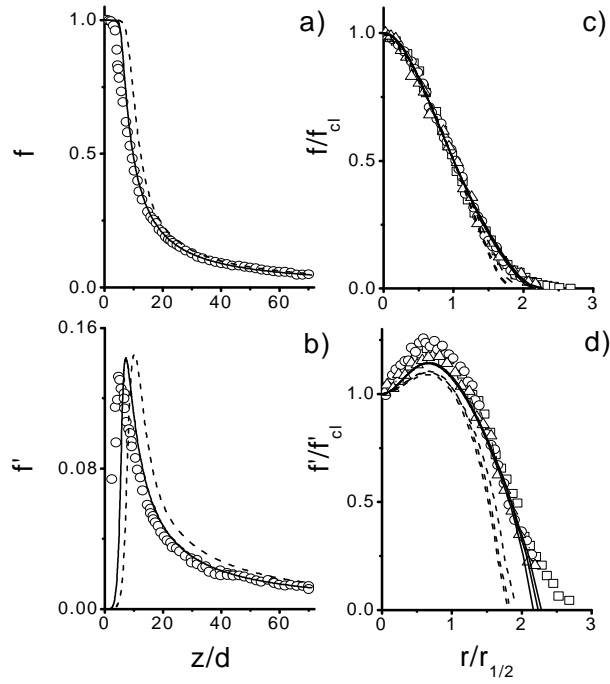


Figure 5. Measured and predicted mean and r.m.s. mixture fraction profiles for Birch et al. jet: a) axial f ; b) axial f' ; c) radial f ; d) radial f' (circles – data, solid line – k - ϵ model, dashed line – second moment closure).

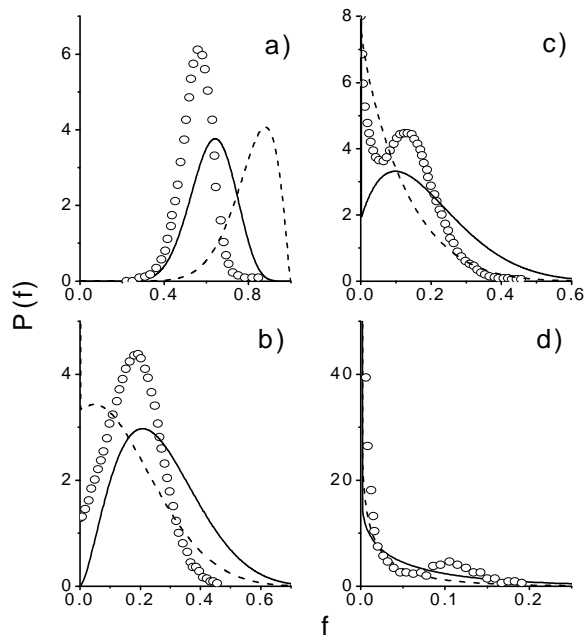


Figure 6. Measured mixture fraction p.d.f.'s along radius of Birch et al. jet at $z/d = 10$ and flow model-based predictions: a) $r/d = 0.0$; b) $r/d = 1.3$; c) $r/d = 1.49$; d) $r/d = 1.8$ (key as Figure 5).